



Novel Mechanisms of Valproate Hepatotoxicity: Impaired Mrp2 Trafficking and Hepatocyte Depolarization

Dong Fu ¹, Panli Cardona, Henry Ho, Paul B. Watkins, and Kim L. R. Brouwer ¹

Division of Pharmacotherapy and Experimental Therapeutics, UNC Eshelman School of Pharmacy, University of North Carolina at Chapel Hill, Chapel Hill, North Carolina 27599

¹To whom correspondence should be addressed at Division of Pharmacotherapy and Experimental Therapeutics, UNC Eshelman School of Pharmacy, 301 Pharmacy Lane, University of North Carolina at Chapel Hill, Chapel Hill, NC 27599-7569. Fax: +1 919 962 0644; E-mail: dongfu@email.unc.edu, kbrouwer@unc.edu.

ABSTRACT

Drug-induced liver injury (DILI) remains a major challenge in drug development. Although numerous mechanisms for DILI have been identified, few studies have focused on loss of hepatocyte polarization as a DILI mechanism. The current study investigated the effects of valproate (VPA), an antiepileptic drug with DILI risk, on the cellular mechanisms responsible for loss of hepatocyte polarization. Fully polarized collagen sandwich-cultured rat hepatocytes were treated with VPA (1–20 mM) for specified times (3–24 h). Hepatocyte viability was significantly decreased by 10 and 20 mM VPA. Valproate depolarized hepatocytes, even at noncytotoxic concentrations (≤ 5 mM). Depolarization was associated with significantly decreased canalicular levels of multidrug resistance-associated protein 2 (Mrp2) resulting in reduced canalicular excretion of the Mrp2 substrate carboxydichlorofluorescein. The decreased canalicular Mrp2 was associated with intracellular accumulation of Mrp2 in Rab11-positive recycling endosomes and early endosomes. Mechanistic studies suggested that VPA inhibited canalicular trafficking of Mrp2. This effect of VPA on Mrp2 appeared to be selective in that VPA had less impact on canalicular levels of the bile salt export pump (Bsep) and no detectable effect on P-glycoprotein (P-gp) canalicular levels. Treatment with VPA for 24 h also significantly downregulated levels of tight junction (TJ)-associated protein, zonula occludens 2 (ZO2), but appeared to have no effect on the levels of TJ proteins claudin 1, claudin 2, occludin, ZO1, and ZO3. These findings reveal that two novel mechanisms may contribute to VPA hepatotoxicity: impaired canalicular trafficking of Mrp2 and disruption of ZO2-associated hepatocyte polarization.

Key words: drug-induced liver injury; multidrug resistance-associated protein 2; protein trafficking; hepatocyte polarization; tight junction.

Drug-induced liver injury (DILI) is a mechanistically multifactorial event. Direct hepatocellular injury and immune-mediated injury are the two major causes of DILI (Mosedale and Watkins, 2017; Yuan and Kaplowitz, 2013). Hepatocellular injury is often associated with altered activity of metabolic enzymes and/or impaired function of efflux transporters. These changes may result in cellular accumulation of endogenous substances, drugs, and/or metabolites, leading to hepatocellular stress and injury

(Swift *et al.*, 2010; Tujios and Fontana, 2011), and consequently, cell death.

Transporters, especially efflux transporters, are essential for hepatic detoxification. Efflux transporters help maintain non-toxic cellular levels of xenobiotics and metabolites, thus preventing hepatocellular injury (Kock and Brouwer, 2012). Hepatocytes have a well-defined polarized architecture, a fundamental morphology that supports the efflux and influx

functions of transporters (Gissen and Arias, 2015). Polarized hepatocytes have distinct apical (canalicular) and basolateral membranes that are segregated by tight junctions (TJs). The bile canaliculus, a tubular structure formed by apical membranes of adjacent hepatocytes, connects with other canaliculi to form a canalicular network, into which bile acids, drugs, and metabolites are secreted. The basolateral membrane, which faces the space of Disse, facilitates the exchange of biological materials and xenobiotics with sinusoidal blood (Treyer and Musch, 2013).

The key determinants of hepatocyte polarization are functional polarization and structural polarization (Gissen and Arias, 2015). Functional polarization is associated with the cellular localization and function of canalicular and basolateral transporters. The three major ATP-binding cassette (ABC) transporters located on the canalicular membrane are the bile salt export pump (BSEP; ABCB11), P-glycoprotein (P-gp; ABCB1), and multidrug resistance-associated protein 2 (MRP2; ABCG2). These transporters are efflux pumps that remove chemically and pharmacologically distinct substrates from hepatocytes, and are essential for functional polarization (Kock and Brouwer, 2012). Disruption of functional polarization leads to impaired efflux of endogenous/exogenous substrates. Structural polarization includes the integrity of TJs and the formation of bile canaliculi (Shin et al., 2006; Zihni et al., 2016). Tight junction proteins consist of two major types of transmembrane proteins, claudin and occludin, and three main TJ-associated proteins, zonula occludens (ZO1, 2, and 3) (Zihni et al., 2016). ZO1, 2, and 3 are involved in association of claudin and occludin with the cytoskeleton and other cellular organelles/proteins. Disruption of TJs causes structural depolarization and hepatocellular injury. For example, Type 4 progressive familial intrahepatic cholestasis is caused by a homozygous mutation in ZO2 (Gissen and Arias, 2015). ZO2 deficiency is also associated with the development of hepatocellular carcinoma in childhood (Zhou et al., 2015).

Our recent results revealed that hepatotoxic drugs, acetaminophen (APAP) and diclofenac, caused depolarization in both collagen sandwich-cultured rat and human hepatocytes (Kang et al., 2016). Even at low and nontoxic doses, APAP depolarized hepatocytes by disrupting TJ integrity, leading to cellular stress (Gamal et al., 2017). In a more recent study, alpha-naphthyl isothiocyanate altered TJ permeability and the levels of bile acid transporters in rats, resulting in hepatocyte depolarization before the development of cholestatic hepatotoxicity (Yang et al., 2017). These studies indicate that disruption of hepatocyte polarization could be a causal factor in DILI. However, detailed insights are still lacking regarding how hepatotoxic drugs impair functional and/or structural polarization of hepatocytes. In the current study, valproate (VPA) is used as a model drug to investigate drug-induced alterations in hepatocyte polarization and how these changes may lead to cellular stress and injury.

Valproate, an antiepileptic drug used to treat seizures, bipolar disorder, and anxiety, is metabolized in the liver by glucuronidation (50%), mitochondrial β -oxidation (40%), and cytochrome P450 (CYP)-mediated oxidation (10%) (Ghodke-Puranik et al., 2013). Damage to the liver and pancreas are the most common adverse reactions in patients administered VPA. A black box warning for hepatotoxicity is included in the VPA label (Tujios and Fontana, 2011). The therapeutic serum concentration range of VPA is 0.35–0.875 mM, and toxicity can occur when serum concentrations are >1.05 mM (Ghannoum et al., 2015). Valproate hepatotoxicity has been attributed, in part, to

inhibition of mitochondrial β -oxidation (Ghodke-Puranik et al., 2013). However, the mechanism(s) underlying VPA hepatotoxicity (e.g., mitochondrial dysfunction, oxidative stress, altered bile acid homeostasis, other unrecognized pathways) have not been completely characterized.

To elucidate the mechanisms contributing to VPA hepatotoxicity, the current study used collagen sandwich-cultured rat hepatocytes (SCRH) to investigate the effect of VPA on hepatocyte polarization. Results revealed that VPA produced both functional depolarization via impaired Mrp2 trafficking and ZO2-associated structural depolarization, which are likely mechanisms contributing to VPA hepatotoxicity.

MATERIALS AND METHODS

Chemicals and reagents. Sodium VPA, cycloheximide (CHX), rat-anti ZO1 antibody, and mouse anti-actin antibody were obtained from Sigma-Aldrich (Carlsbad, California). Rabbit anti-BSEP, rabbit anti-claudin 1, rabbit anti-claudin 2, and rabbit anti-occludin were from Abcam (Cambridge, Massachusetts). Mouse anti-MRP2 antibody was purchased from Kamiya Biomedical (Tukwila, Washington). Mouse anti-P-gp (ABCB1) antibody was obtained from Covance Research (Princeton, New Jersey). Rabbit anti-ZO2, rabbit anti-EEA1, and rabbit anti-Rab11 were purchased from Cell Signaling Technology (Danvers, Massachusetts). Mouse anti-Rab11 was obtained from BD Transduction Laboratory (San Jose, California). Rat anti-ZO1 antibody was obtained from Merck Millipore (Branchburg, New Jersey). Rabbit-anti Na^+/K^+ ATPase was from Santa Cruz Biotechnology (Dallas, Texas). Mouse anti-EEA1, anti-mouse Alexa 488, anti-rabbit Alexa 488, anti-rabbit CY3, anti-mouse-CY3, anti-rat Alexa 488, anti-rat Alexa 633 antibodies, AlamarBlue kit, Pierce cell surface protein isolation kit, bicinchoninic acid (BCA) protein assay kit, and 4',6-diamidino-2-phenylindole (DAPI), 5(6)-carboxy-2', 7'-dichlorofluorescein diacetate (CFDA) were purchased from Thermo Fisher Scientific (Waltham, Massachusetts). Anti-rabbit HRP and anti-mouse HRP-conjugated IgG were obtained from Jackson ImmunoResearch (West Grove, Pennsylvania).

Collagen SCRH. Freshly isolated rat hepatocytes were purchased from Lonza (Walkersville, Maryland). The details for culturing SCRH were described in a recent publication (Fu and Lippincott-Schwartz, 2018). Briefly, 35 mm glass-bottom dishes (MatTek, Ashland, Massachusetts) were coated with Type 1 collagen from rat tail (1.5 mg/ml) (Corning Inc., Corning, New York) followed by seeding 1.95×10^5 rat hepatocytes on the 14 mm glass micro-well. After attachment, hepatocytes were overlaid with Type 1 collagen (1.5 mg/ml). Nonproliferative primary rat hepatocytes were cultured for 6 days until the hepatocytes became fully polarized and formed interconnected bile canaliculi within the culture. SCRH were treated in all experiments starting on day 6 of culture.

Cell viability assays. The AlamarBlue assay kit was used to determine cell viability based on the protocol recommended by the manufacturer. Hepatocytes were treated with or without VPA followed by the addition of AlamarBlue to the culture medium and incubation for 4 h at 37°C. The culture supernatants were used for absorbance measurements at 570 and 600 nm. Cells were lysed and total protein concentration was determined by the BCA assay. The absorbance was normalized for the protein concentration to calculate cell viability.

Immunofluorescence and confocal microscopy. The detailed methods were described previously by Fu et al. (2010) and Kang et al. (2016). Images were taken using a Zeiss 710 confocal microscope with a Plan Achromat 40×/1.4 Oil DIC objective. To quantify canalicular length, at least three images were randomly taken within a field of view. All the images were a merged projection of z-stacks to preserve the 3D canalicular structure. Measurement and calculation of canalicular length were described previously by Fu et al. (2010).

Western blot. After various treatments, hepatocytes were harvested and lysed in radioimmunoprecipitation assay buffer (Thermo Fisher Scientific). The lysates were sonicated on ice using a sonicator (10–12 s with 1 s intervals). Total proteins were extracted by centrifugation (15 000 g for 35 min at 4°C). Protein samples were subjected to separation using NuPage gels (Thermo Fisher Scientific) followed by transferring to polyvinylidene difluoride membranes. Western blot was performed and imaged by ChemiDoc XRS+ imaging system with Image Lab program (Bio-Rad, Hercules, California). Actin was used as a loading control. Details were described previously by Kang et al. (2016).

Biotinylation of cell surface proteins. Biotinylation was performed using Pierce cell surface protein isolation kit following the recommended protocol from the manufacturer. Biotinylation was performed at 4°C to allow biotin binding to surface proteins, including those on the canalicular membrane (Ihrke et al., 1993; Wakabayashi et al., 2004). The biotinylation steps were modified as follows: 0.5 mg/ml of EZ-Link Sulfo-NHS-SS-Biotin was used, samples were incubated for 40 min at 4°C, and the amount of quenching solution was doubled. Biotinylated samples were used for western blot assays. Na⁺/K⁺ ATPase was used as a loading control.

Canalicular accumulation of Mrp2 substrate. Freshly isolated rat hepatocytes (Lonza) were cultured in 24-well plates that were coated with Type 1 rat tail collagen. Hepatocytes were overlaid with 0.25 mg/ml Matrigel (Corning Inc.) diluted in culture medium and cultured for 6 days to achieve fully polarized morphology. 5(6)-Carboxy-2', 7'-dichlorofluorescein diacetate is a nonfluorescent compound that passively diffuses into hepatocytes followed by enzymatic conversion to the fluorescent 5, 6-carboxydichlorofluorescein (CDF). 5, 6-Carboxydichlorofluorescein is a Mrp2 substrate that is predominantly secreted into bile canaliculi by Mrp2 (Chandra et al., 2005). To determine the canalicular secretion of CDF by Mrp2, B-CLEAR[®] technology was used to measure total (cells + bile) and cellular accumulation of CDF; accumulation of CDF in bile was obtained by subtracting the cellular accumulation from the total accumulation (Liu et al., 1999; Swift et al., 2010). Hepatocytes were treated with various concentrations of VPA (0, 1, 2.5, 5, 10, and 20 mM) for 24 h, or 10 mM VPA for specific times (0, 3, 6, 9, 12, and 24 h). After washing with warm calcium containing (standard) or calcium-free (Ca²⁺-free) HBSS buffer (10 s, 2 times), hepatocytes were incubated with standard or Ca²⁺-free HBSS buffers for 10 min at 37°C in a cell culture incubator. After removal of the buffer, hepatocytes were incubated with CDFDA (2 μM in standard HBSS buffer) for 10 min at 37°C in a cell culture incubator. After removal of the CDFDA, hepatocytes were washed with ice-cold standard HBSS buffer three times for 10 s. Cells were lysed using 0.3 ml of 0.5% TritonX-100 in PBS for 60 min at 4°C in the dark. The lysates (200 μl) were used for the measurement of the fluorescent signals (ex488/em519) by BioTek CYTATION3 Image reader (Winooski, Vermont). The lysates also were used for quantification of the protein concentration using

the BCA assay kit, and data were normalized by the protein concentrations. The biliary excretion index (BEI) represents the fraction of the accumulated substrate that was excreted into bile. CDF BEI, expressed as a percentage, was calculated using the following equation: $[(\text{accumulation}_{(\text{cells} + \text{bile})} - \text{accumulation}_{(\text{cells})}) / \text{accumulation}_{(\text{cells} + \text{bile})}] \times 100$ (Liu et al., 1999).

Statistics. All data are presented as mean ± SD. Statistically significant differences denoted as $p < .05$ were determined using one-way ANOVA.

RESULTS

VPA Depolarized Hepatocytes Even at Noncytotoxic Concentrations

To determine the VPA concentration that caused cytotoxicity, cell viability was measured after SCRH were treated with various concentrations of VPA (0, 1, 2.5, 5, 10, and 20 mM) for 24 h. Treatment with VPA at 10 and 20 mM caused significant cytotoxicity, resulting in 84% and 82% viability, respectively, compared with the untreated control (VPA 0 mM) (Fig. 1A). Lower VPA concentrations (1, 2.5, and 5 mM) only caused a slight decrease in viability (98–94%) compared with the control, suggesting minimal cytotoxicity (Fig. 1A). For subsequent studies, VPA concentrations greater than 5 mM were considered to be cytotoxic in SCRH.

Hepatocyte polarization in SCRH treated with designated VPA concentrations starting on day 6 was assessed by examining the morphological structure of canaliculi within the culture and quantified by canalicular length using confocal microscopy images. Treatment with 5, 10, and 20 mM VPA for 24 h resulted in less canaliculi in hepatocyte cultures and significantly decreased canalicular lengths to 78%, 70%, and 55% of that in the untreated control (0 mM), respectively (Figs. 1B and 1C), indicating that 5, 10, and 20 mM of VPA caused depolarization of hepatocytes. In contrast, treatment with 1 and 2.5 mM VPA did not significantly decrease canalicular lengths (~89% of the untreated control; Figs. 1B and 1C), suggesting that these noncytotoxic VPA concentrations had a modest impact on hepatocyte polarization.

Given that 10 mM VPA caused significant cytotoxicity and hepatocyte depolarization, the effect of 10 mM VPA on hepatocyte polarization was examined further over various exposure times (0, 3, 6, 9, 12, and 24 h). Polarization, as assessed by canalicular length, remained stable in untreated control SCRH during the 24 h period (Supplementary Figs. 1A and 1B). In contrast, VPA treatment progressively decreased canalicular length as early as 3 h (88% of 0 h); VPA treatment for 24 h decreased canalicular length to 66% of 0 h (Figs. 1D and 1E). These data demonstrated that VPA impaired hepatocyte polarization after a short duration of exposure. Subsequent studies to elucidate the mechanism(s) of VPA hepatotoxicity used 10 mM VPA.

VPA Decreased Protein Levels of Major Apical Transporters and Inhibited Apical Trafficking of Mrp2

Apical transporters such as Bsep, Mrp2, and P-gp play major roles in drug disposition and detoxification, and are critical components of functional hepatocyte polarization. Thus, the effects of VPA on protein levels of Bsep, Mrp2, and P-gp were investigated. Hepatocytes were treated with VPA (10 mM) for various times (0, 3, 6, 9, 12, and 24 h). Using total protein extraction, western blot results showed that total Bsep, Mrp2, and P-gp protein levels in the untreated control hepatocytes

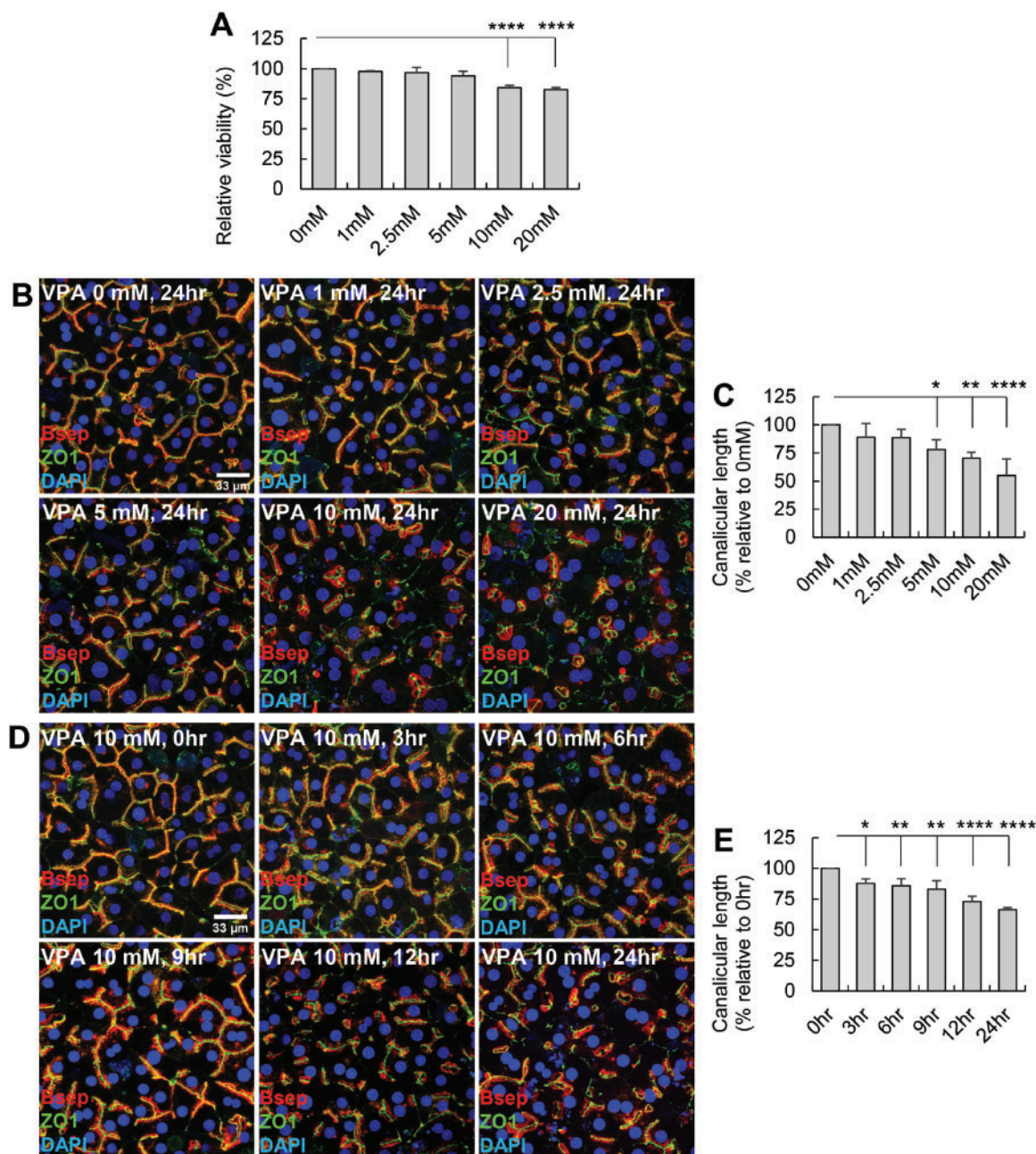


Figure 1. Effects of VPA on viability and polarization of collagen SCRH. **A**, Collagen SCRH were treated with various concentrations of VPA for 24 h (0, 1, 2.5, 5, 10, and 20 mM). AlamarBlue assay showed that low VPA concentrations (1, 2.5, and 5 mM) did not cause significant changes in viability, whereas 10 and 20 mM VPA significantly decreased viability. **B**, SCRH were treated with various concentrations (0, 1, 2.5, 5, 10, and 20 mM) of VPA for 24 h. Confocal microscopy images with immunostaining for apical (Bsep) and TJ (ZO1) markers and nuclear staining (DAPI) showed that VPA caused concentration-dependent depolarization of hepatocytes with less branched canalicular networks. **C**, VPA significantly reduced canaliculus length of hepatocytes, even at a noncytotoxic concentration (5 mM). **D** and **E**, SCRH were treated with 10 mM VPA for specific times (0, 3, 6, 9, 12, and 24 h). Valproate caused hepatocyte depolarization and decreased canaliculus length even after short-term exposure (3 h). Valproate treatment caused the most depolarization at 12 and 24 h. * $p < .05$, ** $p < .01$, **** $p < .0001$ compared with 0 mM or 0 h; $n = 3-4$. Abbreviations: SCRH, sandwich-cultured rat hepatocytes; VPA, valproate; TJ, tight junction; Bsep, bile salt export pump; ZO1, zonula occludens 1; DAPI, 4',6-diamidino-2-phenylindole.

(CTRL) remained steady within the 24 h treatment period (Supplementary Figs. 1C-E). Mrp2 and Bsep protein levels trended lower at 24 h after VPA treatment, but due to experimental variability, differences were not statistically significant at any time point (Figs. 2A and 2B). Valproate had no significant effect on P-gp protein levels at any time point (Fig. 2C).

To determine whether VPA altered the levels of canaliculus transporters already localized on the apical membrane, biotinylation of surface proteins was performed. Using the biotinylated

samples, western blot analysis showed that VPA treatment progressively decreased canaliculus Mrp2 protein levels, resulting in 82% at 3 h, 64% at 6 h, 46% at 9 h, and 39% at 12 h and 24 h relative to the 0 h time point (Fig. 2D). Valproate did not significantly alter canaliculus levels of Bsep or P-gp (Figs. 2E and 2F).

To further evaluate the effect of VPA on canaliculus localization/trafficking of Mrp2, Bsep, and P-gp, immunofluorescent tagging of Mrp2, Bsep, and P-gp was performed after hepatocytes were treated with 10 mM VPA for various times (0-24 h).

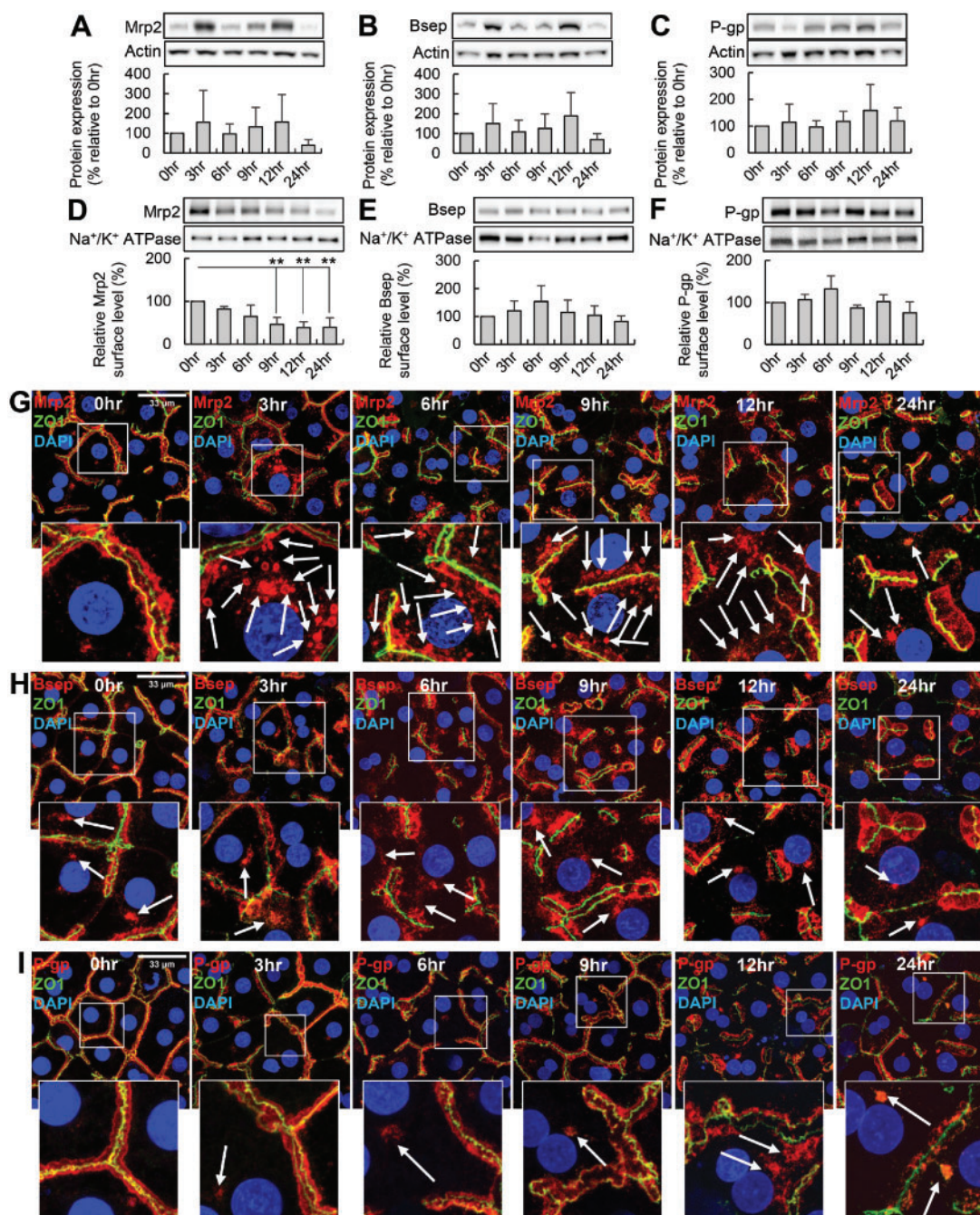


Figure 2. Effect of VPA on protein levels and canalicular localization of Mrp2, Bsep and P-gp. SCRHe were treated with 10 mM VPA for specific times (0, 3, 6, 9, 12, and 24 h). Total protein levels were detected by western blot (A–C). Levels of canalicular Mrp2, Bsep, and P-gp were detected by western blot after biotinylation (D–F). Immunofluorescence of Mrp2, Bsep, P-gp, and ZO1 was performed; DAPI was used for nuclear staining. The smaller images are a magnification (3.5–4×) of the areas indicated by the white squares. White arrows indicate intracellularly localized Mrp2, Bsep, and P-gp (G–I). A, VPA reduced Mrp2 protein at 24 h to 40% of control values ($n = 4$). B, VPA only moderately reduced Bsep protein at 24 h to 70% of control values ($n = 4$). C, VPA had no notable impact on P-gp protein levels ($n = 4$). D, VPA significantly decreased canalicular levels of Mrp2 at 9, 12, and 24 h (** $p < .01$, compared with 0 h; $n = 3$). E, VPA did not significantly change canalicular levels of Bsep ($n = 3$), or F, P-gp ($n = 3$). G, VPA exposure (3–24 h) increased intracellular accumulation of Mrp2, which was located primarily in vesicle-like structures around the sub-canalicular regions of hepatocytes; intracellular Mrp2 was less notable at 24 h. H, Intracellular accumulation of Bsep was moderately increased in hepatocytes treated with VPA (3–24 h). Intracellular Bsep was located primarily in perinuclear and cytosolic regions. I, VPA did not increase intracellular accumulation of P-gp after 3–12 h. After treatment with VPA for 24 h, some intracellular accumulation of P-gp was observed around the perinuclear regions. Abbreviations: VPA, valproate; SCRHe, sandwich-cultured rat hepatocytes; Bsep, bile salt export pump; Mrp2, multidrug resistance-associated protein 2; P-gp, P-glycoprotein; ZO1, zonula occludens 1; DAPI, 4',6'-diamidino-2-phenylindole.

The confocal microscopy data revealed that Mrp2, Bsep, and P-gp were predominantly localized on the canalicular membrane in untreated CTRL at 0, 3, 6, 9, 12, and 24 h (Supplementary Figs. 2A–C). In contrast, VPA treatment caused intracellular accumulation of Mrp2 at 3 h in a majority of the hepatocytes (Fig. 2G). The accumulated intracellular Mrp2 was located primarily in the sub-apical region, and appeared as vesicles in many cases, indicating that VPA inhibits Mrp2 trafficking to the canalicular membrane and/or causes Mrp2 internalization (Fig. 2G). The increased intracellular accumulation of Mrp2 became less notable at 24 h treatment. In contrast, VPA only moderately increased intracellular accumulation of Bsep, which was located primarily around the perinuclear region (Fig. 2H). No apparent change in intracellular accumulation of P-gp occurred after VPA treatment (Fig. 2I). These data reveal for the first time that impaired Mrp2 apical trafficking/localization is a mechanism associated with VPA hepatotoxicity.

Intracellular Accumulation of Mrp2 Was Localized Primarily in Endosomal Compartments

Apical transporters traffic to the canalicular membrane through the endosomal pathway (Fu, 2013). To identify where the intracellular accumulation of Mrp2 was localized, co-localization assays were performed using the early endosomal marker, EEA1, and the recycling endosomal marker, Rab11. Hepatocytes were treated with VPA (10 mM) for various times. Immunofluorescence and confocal microscopy results showed that Mrp2 was largely co-localized with canalicular marker ZO1 at the beginning of the treatment (0 h) (Fig. 3A), indicating Mrp2 is predominantly localized on canaliculi, as expected. Some Mrp2 was localized intracellularly and was co-localized with Rab11 (Fig. 3A). Notably, Rab11-positive recycling endosomes (RE) were localized at both perinuclear and sub-canalicular regions. The sub-canalicular Rab11-positive RE were in very close proximity to the apical membrane (Fig. 3A). The close proximity of Rab11 to the canalicular membrane was also reported in previous studies in both rat liver tissues and hepatocyte cultures (Gupta et al., 2016; Rahner et al., 2000). Valproate treatment (3 h) caused more intracellular Mrp2 to accumulate in the sub-canalicular region (Fig. 3B), and the sub-canalicular Mrp2 was largely co-localized with Rab11 (Fig. 3B).

The intracellular Mrp2 that was not co-localized with Rab11 was further identified by immunostaining with the early endosome marker EEA1. At the beginning of treatment (0 h), Mrp2 was largely localized on canaliculi (Fig. 3C) and only a small amount of intracellular Mrp2 was co-localized with EEA1 at the perinuclear region (Fig. 3C). After VPA treatment (3 h), some of the intracellular Mrp2 was co-localized with EEA1 at both perinuclear and sub-canalicular regions (Fig. 3D), suggesting intracellular Mrp2 was also localized in early endosomes (EE). In addition, time course results also showed that increased intracellular Mrp2 was predominantly localized at both EE and RE at the early stage of VPA treatment (3–9 h) (Supplementary Figs. 3 and 4). Taken together, these data reveal that VPA disrupted endosomal trafficking of Mrp2, leading to Mrp2 accumulation in both EE and RE.

Inhibition of Protein Synthesis Prevented VPA-Mediated Intracellular Accumulation of Mrp2

To further investigate the hypothesis that VPA disrupted newly synthesized Mrp2 from trafficking to the canalicular membrane, hepatocytes were first treated with the protein synthesis inhibitor, CHX (10–100 µg/ml, 5 h), followed by the addition of VPA

(10 mM, 3 h). The cellular accumulation of Mrp2 was examined by immunofluorescence and confocal microscopy. Cycloheximide prevented VPA-mediated intracellular accumulation of Mrp2 in a concentration-dependent manner (Fig. 4).

VPA Decreased the Protein Levels of TJ Protein ZO2 and Disrupted Structural Polarization of Hepatocytes

Given that TJ proteins are essential for maintenance of the polarized morphology, the effects of VPA on TJ proteins were examined. The protein levels of claudin 1 and claudin 2, the main isoforms in liver (Gunzel and Yu, 2013), and occludin were examined after SCRH were treated with VPA (10 mM) for various times (0, 3, 6, 9, 12, and 24 h). Western blot results showed that VPA treatment significantly decreased protein levels of ZO2 at 24 h (27% compared with 0 h; Fig. 5F), but did not significantly alter the levels of other major TJ proteins, including claudin 1, claudin 2, occludin, ZO1, and ZO3 (Figs. 5A–E).

The cellular localization of ZO2 was also examined after VPA treatment. Results showed that ZO2 was located predominantly along canaliculi in the untreated control cells, and primarily remained localized to the canalicular domain or sub-canalicular region after short-term exposure to VPA (3–9 h). However, intracellular localization of ZO2 increased when hepatocytes were treated with VPA (Fig. 5G). These data suggest that VPA reduced canalicular-associated ZO2 resulting in internalization and possible degradation of ZO2, which may contribute to hepatocyte depolarization. Notably, immunostaining showed that ZO1 largely remained either on the canaliculi or on the plasma membrane outside canaliculi, likely the lateral membranes, after treatment with VPA for 24 h (Supplementary Fig. 5A), indicating that VPA did not impact membrane localization of ZO1.

VPA Inhibited Canalicular Accumulation of a Mrp2 Substrate

To ensure that inhibition of Mrp2 trafficking and consequent depolarization of hepatocytes impaired canalicular secretion of Mrp2, the canalicular accumulation of a Mrp2 substrate, CDF (Fig. 6A), was examined in the presence and absence of VPA. The collagen-Matrigel SCRH had similar canalicular network formation (Fig. 6A) and similar protein levels of Bsep, Mrp2, and P-gp compared with the collagen-collagen SCRH (Supplementary Fig. 5B). Using B-CLEAR® technology, the accumulation of CDF in “cells + bile” and “cells” of SCRH was measured, and the BEI was calculated as detailed in the Methods. Valproate (10 and 20 mM) decreased the biliary excretion of CDF; the BEI decreased from 41% to 18% and 11%, respectively (Fig. 6B). Furthermore, 10 mM VPA treatment for 24 h progressively decreased the BEI of CDF from 41% to 18% (Fig. 6C). Taken together, these results confirm that disruption of Mrp2 trafficking as well as hepatocyte depolarization by VPA impaired canalicular secretion of CDF by Mrp2.

DISCUSSION

The current study reveals two novel mechanisms that may contribute to VPA hepatotoxicity. First, VPA inhibited apical trafficking of Mrp2 resulting in increased intracellular accumulation of Mrp2 and decreased canalicular localization of Mrp2; these changes led to impaired Mrp2-mediated canalicular excretion (Fig. 7). Secondly, VPA reduced ZO2 protein levels, causing TJ disruption and hepatocyte depolarization (Fig. 7). This emphasizes the multifactorial nature of DILI, and suggests that individuals with a pathological or acquired condition that impacts one of these targets/pathways may exhibit increased

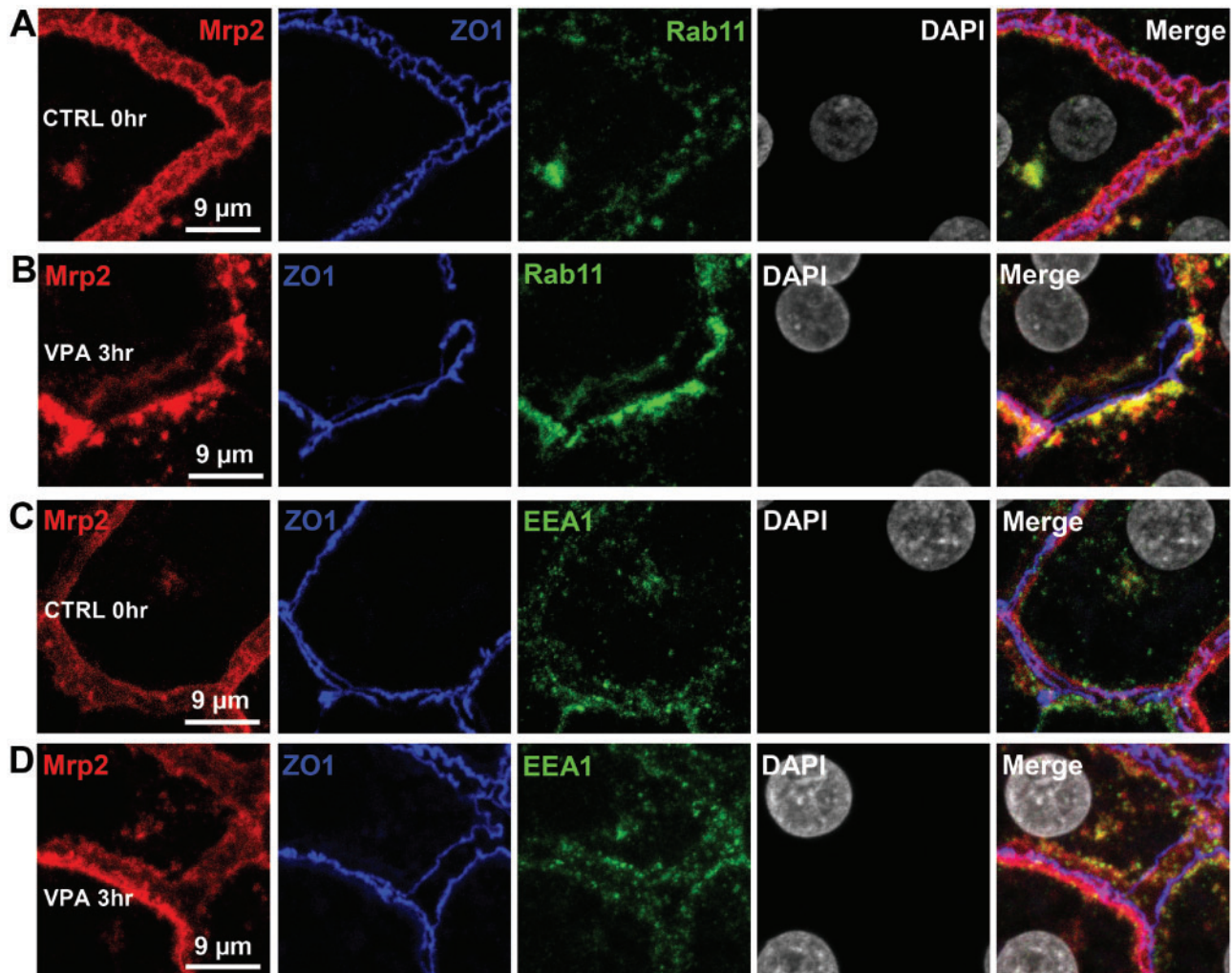


Figure 3. Co-localization of intracellular Mrp2 with the recycling endosomal marker Rab11 and the early endosomal marker EEA1 after VPA treatment. SCRH were treated with 10 mM VPA for 3 h. Immunofluorescence of Mrp2 (red), ZO1 (blue), and Rab11 (green) or EEA1 (green) was performed. Nuclei were stained with DAPI (white). The projection images of the z-stacks for individual and merged channels are presented. **A**, Co-localization of Mrp2 with ZO1 and Rab11 in the CTRL. Mrp2 was primarily co-localized with ZO1 (merged as purple color), indicating the canalicular localization. Rab11 was localized at both sub-canalicular and perinuclear regions. Intracellular Mrp2 was co-localized with Rab11 (merged as yellow/orange color). **B**, Co-localization of Mrp2 with ZO1 and Rab11 in the hepatocytes treated with 10 mM VPA (3 h). Intracellular Mrp2 (red) was primarily localized at the sub-canalicular region. Large amounts of Rab11 were also localized at the sub-canalicular region. Intracellular Mrp2 was primarily co-localized with Rab11 (merged as yellow/orange color). **C**, Co-localization of Mrp2 with ZO1 and EEA1 in the CTRL. Mrp2 was primarily co-localized with ZO1 (merged as purple color), indicating the canalicular localization. EEA1 was localized at both sub-canalicular and perinuclear regions. Intracellular Mrp2 was co-localized with EEA1 primarily in the perinuclear region (merged as yellow/orange color). **D**, Co-localization of Mrp2 with ZO1 and EEA1 in the hepatocytes treated with 10 mM VPA (3 h). Intracellular Mrp2 was primarily localized in the sub-canalicular region. The canalicular localized Mrp2 was co-localized with ZO1 (merged as purple color). Intracellular Mrp2 was co-localized with EEA1 (merged as yellow/orange color). Abbreviations: CTRL, control hepatocytes; VPA, valproate; SCRH, sandwich-cultured rat hepatocytes; Mrp2, multidrug resistance-associated protein 2; ZO1, zonula occludens 1; EEA1, early endosome antigen 1; Rab11, Ras-related protein Rab-11; DAPI, 4',6-diamidino-2-phenylindole.

susceptibility to DILI. Although the 10 mM VPA concentration is higher than therapeutic serum concentrations, hepatocellular concentrations achieved in patients who experience VPA hepatotoxicity have not been reported. A previous study showed that VPA reduced SCRH viability at 1 mM, and caused significant cytotoxicity (Lactate Dehydrogenase assay) at 6 mM; however, these SCRH were cultured for a much shorter period of time, which might explain differences in sensitivity to drug toxicity (Kiang et al., 2010).

Valproate hepatotoxicity has been associated with mitochondrial toxicity, including inhibition of β -oxidation, impaired oxidative phosphorylation, and reduced adenosine triphosphate synthesis (Nanau and Neuman, 2013; Tong et al., 2005). Given that VPA impaired trafficking of Mrp2, but not Bsep or P-

gp, inhibition of β -oxidation is unlikely to be the cause of impaired Mrp2 trafficking. Valproate and/or VPA metabolites may target specific regulator(s) of Mrp2 trafficking, leading to inhibition of Mrp2 canalicular trafficking and consequently, accumulation of toxic Mrp2 substrates that target various cellular pathways including mitochondria.

Valproate caused Mrp2 to accumulate predominantly in EE and RE; this effect could be due to internalization of Mrp2 from the canalicular membrane, or inhibition of canalicular trafficking of newly synthesized protein. Given that the half-life of fully glycosylated rat Mrp2 protein is approximately 45 h in SCRH (Zhang et al., 2005), any Mrp2 that has internalized due to VPA would still be in the endosomal compartments at early time points (e.g., 3 h) in the presence of the protein synthesis

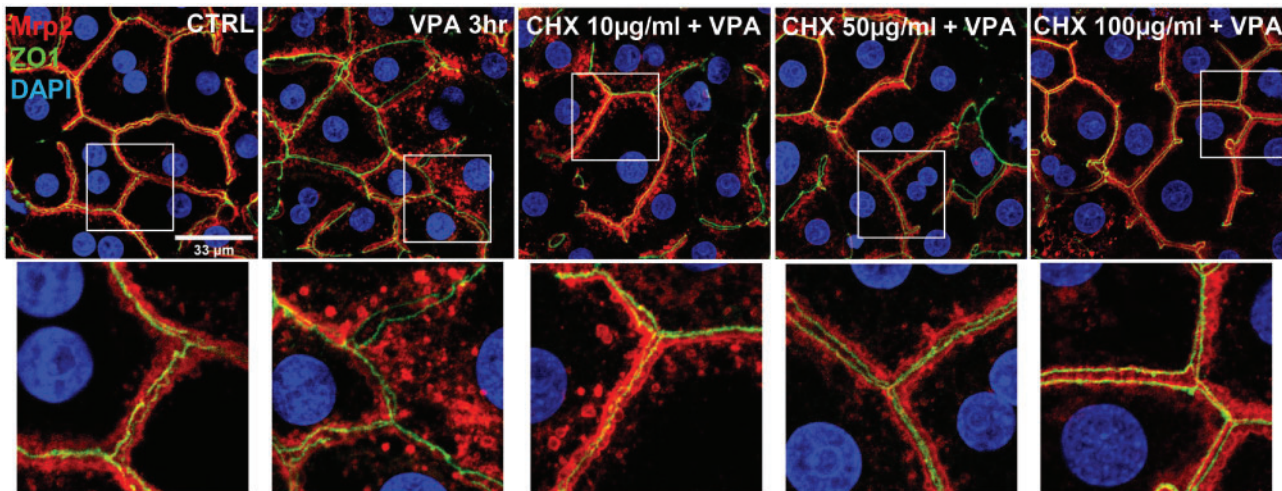


Figure 4. Inhibition of protein synthesis prevented VPA-mediated intracellular accumulation of Mrp2. SCRH were treated with 10, 50, or 100 µg/ml of CHX for 5 h prior to addition of VPA (10 mM) for 3 h. Immunofluorescence localization of Mrp2 and ZO1 was examined by confocal microscopy. The smaller images are a magnification ($\times 3.5$) of the areas indicated by the white squares. Abbreviations: CHX, cycloheximide; VPA, valproate; SCRH, sandwich-cultured rat hepatocytes; Mrp2, multidrug resistance-associated protein 2; ZO1, zonula occludens1; DAPI, 4',6'-diamidino-2-phenylindole.

inhibitor CHX. However, treatment with VPA (3 h) in the presence of CHX led to very little intracellular Mrp2 (Fig. 4). Therefore, the intracellular Mrp2 after VPA (3 h) exposure may be attributed to Mrp2 that did not traffic to the canalicular membrane after synthesis and posttranslational modification. These data support the hypothesis that VPA first inhibits canalicular trafficking of Mrp2, followed by disruption of the ZO2-associated TJ pathway and impaired polarization, leading to hepatotoxicity.

Rab proteins are small GTPases that play a critical role in regulating trafficking of apical transporters (Fu, 2013). Rab11 is localized on apical RE (Welz et al., 2014), and VPA-mediated accumulation of Mrp2 was predominantly at Rab11-positive RE. A previous study also demonstrated the involvement of Rab11 in plasma membrane trafficking of MRP2 in sodium/taurocholate co-transporting polypeptide transporter-overexpressing Huh-7 cells (Park et al., 2014). Interestingly, Rab11-positive RE are also involved in apical trafficking of Bsep (Hanley et al., 2017; Wakabayashi et al., 2005). Given that VPA inhibited Mrp2 trafficking and had much less impact on Bsep trafficking, it appears that VPA targets Rab11 effectors that are specifically involved in Mrp2 trafficking. This idea is also consistent with the minimal effect VPA had on canalicular trafficking of P-gp. Rab11 can interact with diverse types of proteins through its downstream effector proteins (Jing and Prekeris, 2009; Prekeris et al., 2000; Wu et al., 2005). Currently, it is unclear whether VPA targets any of these Rab11 effectors for Mrp2 trafficking in hepatocytes.

The impact of VPA on structural depolarization due to a reduction in ZO2 protein levels, but not other major transmembrane TJ proteins (i.e., claudin1, claudin2, occludin) is interesting. Zona occludens (ZO) proteins interact with the transmembrane TJ proteins (i.e., occludin and claudins) to form the TJ complex. As the cytosolic component of the TJ complex, ZO proteins can interact with other cytoplasmic proteins, especially cytoskeletal proteins (Cordenonsi et al., 1999; Zimmerman et al., 2013). Further investigations are needed to elucidate the pathways responsible for VPA-mediated structural depolarization, especially related to these ZO-associated cytoplasmic proteins.

An important aspect of regulating ZO2-associated TJ integrity and Mrp2 trafficking is phosphorylation of ZO2, Mrp2 and possibly their regulatory proteins, such as Rab11 effectors. Protein kinases, especially protein kinase C (PKC) and protein kinase A (PKA, also known as cyclic adenosine monophosphate-dependent protein kinase), play critical roles in protein phosphorylation (Anwer, 2014; Seino and Shibasaki, 2005). There are many isoforms of PKC, and rat hepatocytes express PKC α , PKC δ , PKC ϵ , and PKC ζ (Anwer, 2014). Valproate has been shown to have inhibitory effects on PKC activity in vitro and in vivo (Chen et al., 1994; Saxena et al., 2017). Thus, the effects of VPA on both Mrp2 trafficking and the ZO2-associated TJ complex are likely associated with PKCs, and further studies are needed to elucidate the specific mechanisms.

When VPA inhibits PKCs and/or PKA, the cellular consequences such as inhibition of Mrp2 trafficking and disruption of TJs could occur simultaneously. However, as revealed in the present studies, significant TJ disruption occurred later than the inhibition of Mrp2 trafficking. This may be due to the compensatory machinery for TJ maintenance. Many TJ proteins appear to have redundant functions (Sambrotta and Thompson, 2015), which may explain why ZO1 largely remained on the membrane after VPA treatment (Supplementary Fig. 5A). Knockout or knockdown of single TJ-associated proteins in cells and in whole organisms often yielded only minimal functional consequences due to adaptive processes in the TJ protein complex when defects of individual components occur in humans (Gonzalez-Mariscal et al., 2017; Sambrotta and Thompson, 2015). Interestingly, the compensatory mechanism for TJ proteins was considered less effective in the liver than in other organs. For example, in patients with ZO2 deficiency, the liver was the major organ damaged, although extrahepatic disorders also occurred, suggesting that ZO2 has a nonredundant role in hepatocyte TJs (Sambrotta and Thompson, 2015).

Reduction in the canalicular localization of Mrp2 by VPA is likely responsible, at least in part, for the cellular responses that lead to further depolarization. At early time points (3–6 h), hepatocyte viability was not significantly decreased when intracellular accumulation of Mrp2 was increased, indicating that decreased apical levels of Mrp2 alone did not immediately cause

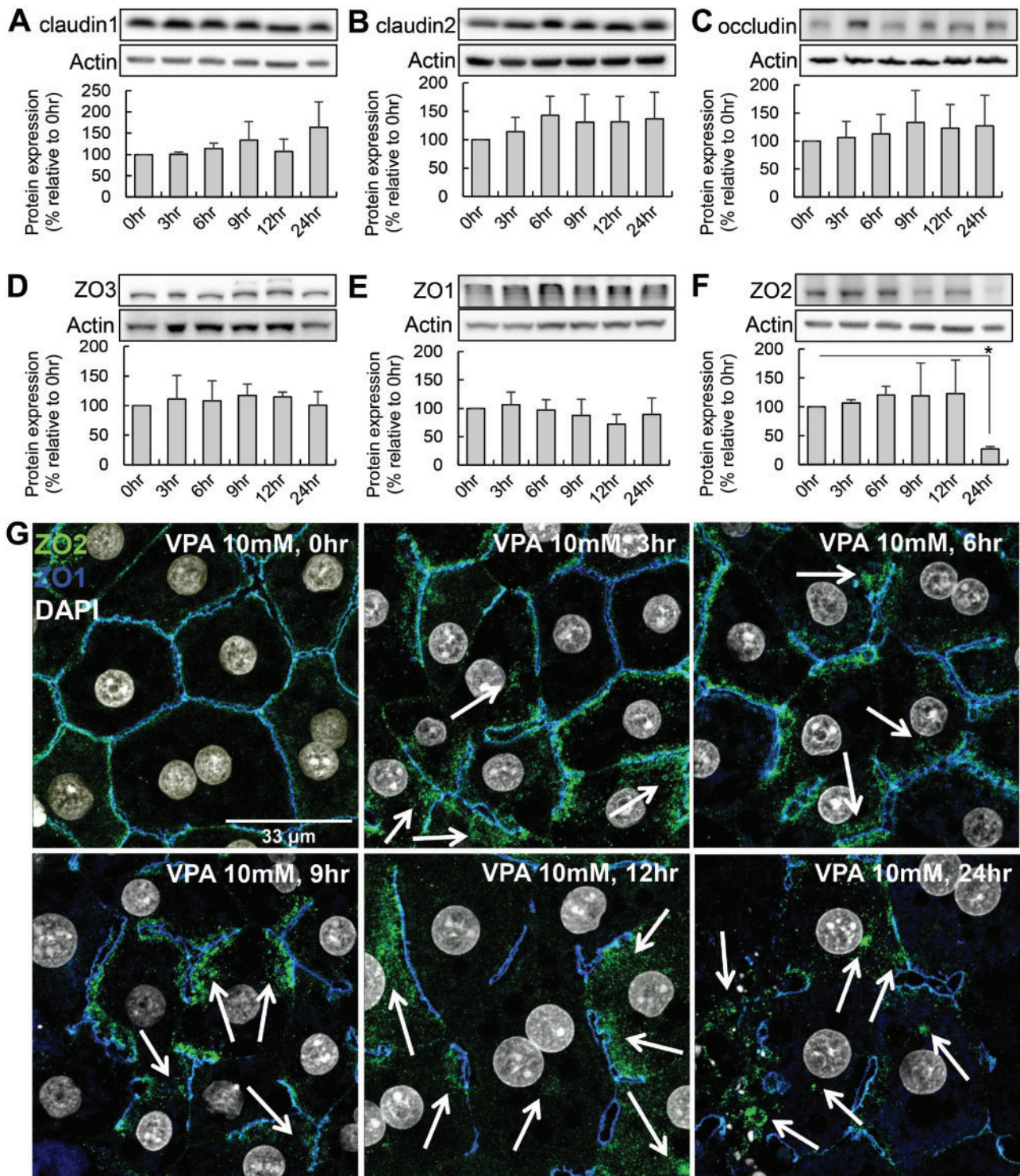


Figure 5. Effect of VPA on TJ protein levels and cellular localization of ZO2. SCRH were treated with 10 mM VPA for specific times (0, 3, 6, 9, 12, and 24 h). Total protein levels were measured by western blot. A–C, VPA did not significantly alter the protein levels of major transmembrane TJ proteins, claudin1, claudin2, or occludin ($n = 3$ –5). D and E, VPA did not significantly alter the levels of the TJ-associated proteins, ZO3 and ZO1 ($n = 3$). F, VPA significantly decreased ZO2 protein levels at 24 h ($*p < .05$, compared with 0 h; $n = 3$). G, Immunofluorescence of ZO2 (blue) and ZO1 (green) were performed at each time point. White arrows indicate intracellular localization of ZO2. Abbreviations: VPA, valproate; TJ, tight junction; SCRH, sandwich-cultured rat hepatocytes; ZO1, zonula occludens 1; ZO2, zonula occludens 2; ZO3, zonula occludens 3; DAPI, 4',6-diamidino-2-phenylindole.

cytotoxicity. Toxic substrates of Mrp2 may accumulate in the cell and disrupt TJs when Mrp2-mediated excretion is impaired. Valproate is not a substrate for either Mrp2 or P-gp (Baltes et al., 2007). However, Mrp2 is the canalicular transporter for a number

of acyl glucuronides of nafenopin, grepafloxacin, mycophenolic acid, and diclofenac (Regan et al., 2010). It is possible that acyl glucuronides of VPA are also Mrp2 substrates (Brouwer et al., 1993). The impaired canalicular localization of Mrp2 can increase

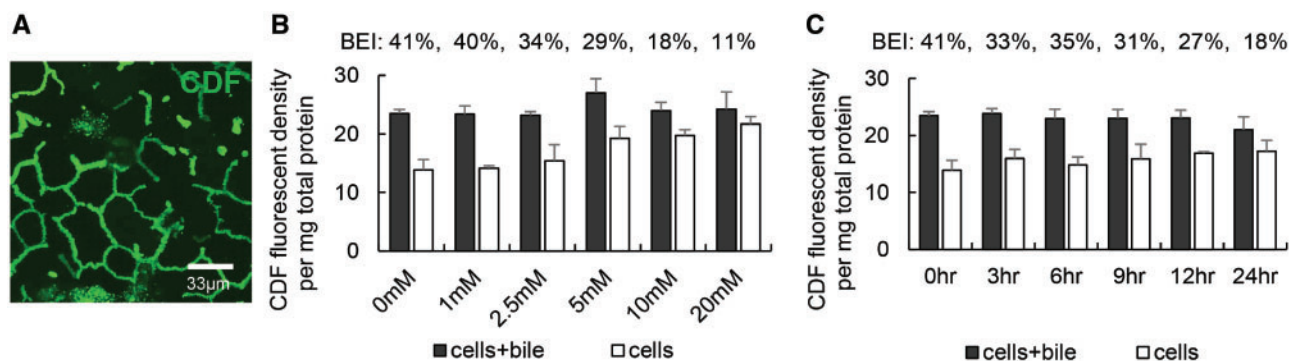


Figure 6. Effect of VPA on canalicular efflux function of Mrp2. A, SCRH were incubated with $2\mu\text{M}$ CDFDA for 10 min. After washing with HBSS, distribution of CDF, the fluorescent metabolite of CDFDA, was imaged by confocal microscopy (ex488/em519). CDF was predominantly secreted into canaliculi. B, SCRH were treated with different concentrations of VPA for 24 h. After incubation with $2\mu\text{M}$ CDFDA for 10 min, accumulation of CDF in cells + bile and cells was examined using B-CLEAR[®] technology, and BEI values were calculated (see Methods for experimental details). Valproate (10 and 20 mM) resulted in 2.3- and 3.7-fold decreases in the BEI of CDF, respectively, compared with 0 mM. C, SCRH were treated with 10 mM VPA for specific times. The BEI of the Mrp2 substrate CDF progressively decreased over time in hepatocytes treated with 10 mM VPA up to a maximal decrease of 2.3-fold at 24 h compared with 0 h. Abbreviations: SCRH, sandwich-cultured rat hepatocytes; CDF, 5(6)-carboxy-2', 7'-dichlorofluorescein; CDFDA, CDF diacetate; BEI, biliary excretion index; VPA, valproate.

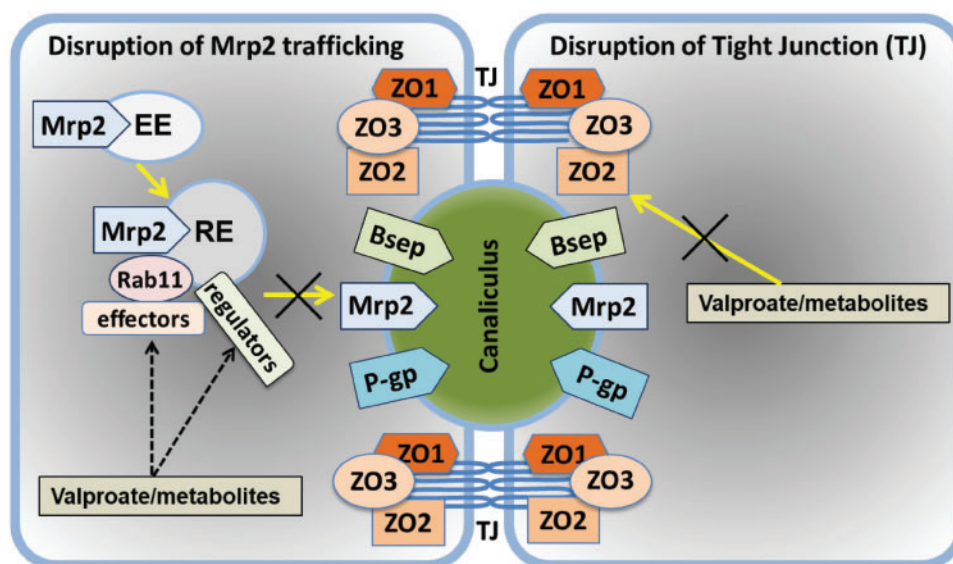


Figure 7. Novel cellular targets and mechanisms involved in VPA hepatotoxicity. Left hepatocyte: VPA and/or VPA metabolites inhibit canalicular trafficking of Mrp2 leading to Mrp2 accumulation at Rab11-positive RE and EE. Valproate and/or VPA metabolites possibly disrupt Mrp2 trafficking either by inhibition of Rab11 effector(s) and/or other regulator(s) for Mrp2 trafficking (black dotted lines). Right hepatocyte: VPA and/or VPA metabolites disrupt ZO2-associated TJ integrity resulting in depolarization. Abbreviations: VPA, valproate; RE, recycling endosomes; EE, early endosomes; TJ, tight junction; Bsep, bile salt export pump; Mrp2, multidrug resistance-associated protein 2; P-gp, P-glycoprotein; ZO1, zonula occludens 1; ZO2, zonula occludens 2; ZO3, zonula occludens 3; Rab11, Ras-related protein Rab-11.

cellular accumulation of various Mrp2 substrates including acyl glucuronides of VPA. However, valproyl 1-O- β -acyl glucuronide, the major glucuronide of VPA generated in SCRH, did not cause toxicity (Surendradoss et al., 2014). Thus, other Mrp2 substrates and/or other VPA metabolites may play major roles in disruption of TJ integrity and hepatocyte polarization.

The present data reveal that inhibition of apical trafficking of Mrp2 and disruption of polarization via down-regulation of ZO2 likely contribute to VPA hepatotoxicity (Fig. 7). Furthermore, impaired functional polarization (i.e., Mrp2 trafficking) preceded disruption of structural polarization. Given that functional and structural polarization are essential for cell function and viability, drug-induced hepatocyte depolarization may play an important role in susceptibility to DILI and may by

itself be a mechanism of DILI. Clearly, VPA can cause hepatotoxicity via multiple cellular targets/mechanisms that ultimately lead to mitochondrial damage and activation of cell death pathways. These cellular targets need to be considered for accurate prediction of DILI risk during drug discovery and development.

SUPPLEMENTARY DATA

Supplementary data are available at Toxicological Sciences online

DECLARATION OF CONFLICTING INTERESTS

Dr. Kim L. R. Brouwer is a co-inventor of the sandwich-cultured hepatocyte technology for quantification of biliary excretion

(B-CLEAR[®]) and related technologies, which have been licensed exclusively to Qualyst Transporter Solutions, LLC, recently acquired by BioIVT. Dr. Kim L.R. Brouwer reports consulting agreements and research grants with several pharmaceutical companies, but none of these represent potential conflicts of interest for this manuscript. Dr. Paul Watkins reports consulting agreements and research grants with several pharmaceutical companies and has a financial interest in DILIsym Services, Inc., but none of these represent potential conflicts for this paper.

ACKNOWLEDGMENTS

We thank the Microscopy Services Laboratory (MSL), UNC Department of Pathology and Laboratory Medicine for the technical support. MSL is supported, in part, by a P30CA016086 Cancer Center Core Support Grant to the UNC Lineberger Comprehensive Cancer Center.

FUNDING

This work was supported by the National Institute of General Medical Sciences of the National Institutes of Health (NIH) [R35 GM122576 to K.L.R.B].

REFERENCES

- Anwer, M. S. (2014). Role of protein kinase C isoforms in bile formation and cholestasis. *Hepatology* **60**, 1090–1097.
- Baltes, S., Fedrowitz, M., Tortos, C. L., Potschka, H., and Loscher, W. (2007). Valproic acid is not a substrate for P-glycoprotein or multidrug resistance proteins 1 and 2 in a number of in vitro and in vivo transport assays. *J. Pharmacol. Exp. Ther.* **320**, 331–343.
- Brouwer, K. L. R., Hall, E. S., and Pollack, G. M. (1993). Protein binding and hepatobiliary distribution of valproic acid and valproate glucuronide in rats. *Biochem. Pharmacol.* **45**, 735–742.
- Chandra, P., Johnson, B. M., Zhang, P., Pollack, G. M., and Brouwer, K. L. R. (2005). Modulation of hepatic canalicular or basolateral transport proteins alters hepatobiliary disposition of a model organic anion in the isolated perfused rat liver. *Drug Metab. Dispos.* **33**, 1238–1243.
- Chen, G., Manji, H. K., Hawver, D. B., Wright, C. B., and Potter, W. Z. (1994). Chronic sodium valproate selectively decreases protein kinase C alpha and epsilon in vitro. *J. Neurochem.* **63**, 2361–2364.
- Cordenonsi, M., D'Atri, F., Hammar, E., Parry, D. A., Kendrick-Jones, J., Shore, D., and Citi, S. (1999). Cingulin contains globular and coiled-coil domains and interacts with ZO-1, ZO-2, ZO-3, and myosin. *J. Cell Biol.* **147**, 1569–1582.
- Fu, D. (2013). Where is it and how does it get there—intracellular localization and traffic of P-glycoprotein. *Front. Oncol.* **3**, 321, 1–5.
- Fu, D., and Lippincott-Schwartz, J. (2018). Monitoring the effects of pharmacological reagents on mitochondrial morphology. *Curr. Protoc. Cell Biol.* **79**, e45.
- Fu, D., Wakabayashi, Y., Ido, Y., Lippincott-Schwartz, J., and Arias, I. M. (2010). Regulation of bile canalicular network formation and maintenance by AMP-activated protein kinase and LKB1. *J. Cell Sci.* **123**, 3294–3302.
- Gamal, W., Treskes, P., Samuel, K., Sullivan, G. J., Siller, R., Srsen, V., Morgan, K., Bryans, A., Kozłowska, A., Koulovasilopoulos, A., et al. (2017). Low-dose acetaminophen induces early disruption of cell-cell tight junctions in human hepatic cells and mouse liver. *Sci. Rep.* **7**, 37541.
- Ghannoum, M., Laliberte, M., Nolin, T. D., Mactier, R., Lavergne, V., Hoffman, R. S., Gosselin, S., and EXTRIP Workgroup. (2015). Extracorporeal treatment for valproic acid poisoning: Systematic review and recommendations from the EXTRIP workgroup. *Clin. Toxicol.* **53**, 454–465.
- Ghodke-Puranik, Y., Thorn, C. F., Lamba, J. K., Leeder, J. S., Song, W., Birnbaum, A. K., Altman, R. B., and Klein, T. E. (2013). Valproic acid pathway: Pharmacokinetics and pharmacodynamics. *Pharmacogenet. Genomics* **23**, 236–241.
- Gissen, P., and Arias, I. M. (2015). Structural and functional hepatocyte polarity and liver disease. *J. Hepatol.* **63**, 1023–1037.
- Gonzalez-Mariscal, L., Miranda, J., Raya-Sandino, A., Dominguez-Calderon, A., and Cuellar-Perez, F. (2017). ZO-2, a tight junction protein involved in gene expression, proliferation, apoptosis, and cell size regulation. *Ann. N. Y. Acad. Sci.* **1397**, 35–53.
- Gunzel, D., and Yu, A. S. (2013). Claudins and the modulation of tight junction permeability. *Physiol. Rev.* **93**, 525–569.
- Gupta, A., Schell, M. J., Bhattacharjee, A., Lutsenko, S., and Hubbard, A. L. (2016). Myosin Vb mediates Cu⁺ export in polarized hepatocytes. *J. Cell Sci.* **129**, 1179–1189.
- Hanley, J., Dhar, D. K., Mazzacuva, F., Fiadeiro, R., Burden, J. J., Lyne, A. M., Smith, H., Straatman-Iwanowska, A., Banushi, B., Virasami, A., et al. (2017). Vps33b is crucial for structural and functional hepatocyte polarity. *J. Hepatol.* **66**, 1001–1011.
- Ihrke, G., Neufeld, E. B., Meads, T., Shanks, M. R., Cassio, D., Laurent, M., Schroer, T. A., Pagano, R. E., and Hubbard, A. L. (1993). WIF-B cells: An in vitro model for studies of hepatocyte polarity. *J. Cell Biol.* **123**, 1761–1775.
- Jing, J., and Prekeris, R. (2009). Polarized endocytic transport: The roles of Rab11 and Rab11-FIPs in regulating cell polarity. *Histol. Histopathol.* **24**, 1171–1180.
- Kang, S. W. S., Haydar, G., Taniane, C., Farrell, G., Arias, I. M., Lippincott-Schwartz, J., and Fu, D. (2016). AMPK activation prevents and reverses drug-induced mitochondrial and hepatocyte injury by promoting mitochondrial fusion and function. *PLoS One* **11**, e0165638.
- Kiang, T. K., Teng, X. W., Karagiozov, S., Surendradoss, J., Chang, T. K., and Abbott, F. S. (2010). Role of oxidative metabolism in the effect of valproic acid on markers of cell viability, necrosis, and oxidative stress in sandwich-cultured rat hepatocytes. *Toxicol. Sci.* **118**, 501–509.
- Kock, K., and Brouwer, K. L. R. (2012). A perspective on efflux transport proteins in the liver. *Clin. Pharmacol. Ther.* **92**, 599–612.
- Liu, X., LeCluyse, E. L., Brouwer, K. R., Gan, L. S., Lemasters, J. J., Stieger, B., Meier, P. J., and Brouwer, K. L. R. (1999). Biliary excretion in primary rat hepatocytes cultured in a collagen-sandwich configuration. *Am. J. Physiol.* **277**, G12–21.
- Mosedale, M., and Watkins, P. B. (2017). Drug-induced liver injury: Advances in mechanistic understanding that will inform risk management. *Clin. Pharmacol. Ther.* **101**, 469–480.
- Nanau, R. M., and Neuman, M. G. (2013). Adverse drug reactions induced by valproic acid. *Clin. Biochem.* **46**, 1323–1338.
- Park, S. W., Schonhoff, C. M., Webster, C. R., and Anwer, M. S. (2014). Rab11, but not Rab4, facilitates cyclic AMP- and tauroursodeoxycholate-induced MRP2 translocation to the plasma membrane. *Am. J. Physiol. Gastrointest. Liver Physiol.* **307**, G863–70.
- Prekeris, R., Klumperman, J., and Scheller, R. H. (2000). A Rab11/Rip11 protein complex regulates apical membrane trafficking via recycling endosomes. *Mol. Cell* **6**, 1437–1448.

- Rahner, C., Stieger, B., and Landmann, L. (2000). Apical endocytosis in rat hepatocytes in situ involves clathrin, traverses a subapical compartment, and leads to lysosomes. *Gastroenterol.* **119**, 1692–1707.
- Regan, S. L., Maggs, J. L., Hammond, T. G., Lambert, C., Williams, D. P., and Park, B. K. (2010). Acyl glucuronides: The good, the bad and the ugly. *Biopharm. Drug Dispos.* **31**, 367–395.
- Sambrotta, M., and Thompson, R. J. (2015). Mutations in TJP2, encoding zona occludens 2, and liver disease. *Tissue Barriers* **3**, e1026537.
- Saxena, A., Scaini, G., Bavaresco, D. V., Leite, C., Valvassoria, S. S., Carvalho, A. F., and Quevedo, J. (2017). Role of protein kinase C in bipolar disorder: A review of the current literature. *Mol. Neuropsychiatry* **3**, 108–124.
- Seino, S., and Shibasaki, T. (2005). PKA-dependent and PKA-independent pathways for cAMP-regulated exocytosis. *Physiol. Rev.* **85**, 1303–1342.
- Shin, K., Fogg, V. C., and Margolis, B. (2006). Tight junctions and cell polarity. *Annu. Rev. Cell Dev. Biol.* **22**, 207–235.
- Surendradoss, J., Chang, T. K., and Abbott, F. S. (2014). Evaluation of in situ generated valproyl 1-O-beta-acyl glucuronide in valproic acid toxicity in sandwich-cultured rat hepatocytes. *Drug Metab. Dispos.* **42**, 1834–1842.
- Swift, B., Pfeifer, N. D., and Brouwer, K. L. R. (2010). Sandwich-cultured hepatocytes: An in vitro model to evaluate hepatobiliary transporter-based drug interactions and hepatotoxicity. *Drug Metab. Rev.* **42**, 446–471.
- Tong, V., Teng, X. W., Chang, T. K., and Abbott, F. S. (2005). Valproic acid II: Effects on oxidative stress, mitochondrial membrane potential, and cytotoxicity in glutathione-depleted rat hepatocytes. *Toxicol. Sci.* **86**, 436–443.
- Treyer, A., and Musch, A. (2013). Hepatocyte polarity. *Compr. Physiol.* **3**, 243–287.
- Tujios, S., and Fontana, R. J. (2011). Mechanisms of drug-induced liver injury: From bedside to bench. *Nat. Rev. Gastroenterol. Hepatol.* **8**, 202–211.
- Wakabayashi, Y., Dutt, P., Lippincott-Schwartz, J., and Arias, I. M. (2005). Rab11a and myosin Vb are required for bile canalicular formation in WIF-B9 cells. *Proc. Natl. Acad. Sci. U.S.A.* **102**, 15087–15092.
- Wakabayashi, Y., Lippincott-Schwartz, J., and Arias, I. M. (2004). Intracellular trafficking of bile salt export pump (ABCB11) in polarized hepatic cells: Constitutive cycling between the canalicular membrane and rab11-positive endosomes. *Mol. Biol. Cell* **15**, 3485–3496.
- Welz, T., Wellbourne-Wood, J., and Kerkhoff, E. (2014). Orchestration of cell surface proteins by Rab11. *Trends Cell Biol.* **24**, 407–415.
- Wu, S., Mehta, S. Q., Pichaud, F., Bellen, H. J., and Quioco, F. A. (2005). Sec15 interacts with Rab11 via a novel domain and affects Rab11 localization in vivo. *Nat. Struct. Mol. Biol.* **12**, 879–885.
- Yang, T., Mei, H., Xu, D., Zhou, W., Zhu, X., Sun, L., Huang, X., Wang, X., Shu, T., Liu, J., et al. (2017). Early indications of ANIT-induced cholestatic liver injury: Alteration of hepatocyte polarization and bile acid homeostasis. *Food Chem. Toxicol.* **110**, 1–12.
- Yuan, L., and Kaplowitz, N. (2013). Mechanisms of drug-induced liver injury. *Clin. Liver Dis.* **17**, 507–518.
- Zhang, P., Tian, X., Chandra, P., and Brouwer, K. L. R. (2005). Role of glycosylation in trafficking of Mrp2 in sandwich-cultured rat hepatocytes. *Mol. Pharmacol.* **67**, 1334–1341.
- Zhou, S., Hertel, P. M., Finegold, M. J., Wang, L., Kerkar, N., Wang, J., Wong, L. J., Plon, S. E., Sambrotta, M., Foskett, P., et al. (2015). Hepatocellular carcinoma associated with tight-junction protein 2 deficiency. *Hepatology* **62**, 1914–1916.
- Zihni, C., Mills, C., Matter, K., and Balda, M. S. (2016). Tight junctions: From simple barriers to multifunctional molecular gates. *Nat Rev Mol Cell Biol* **17**, 564–580.
- Zimmerman, S. P., Hueschen, C. L., Malide, D., Milgram, S. L., and Playford, M. P. (2013). Sorting nexin 27 (SNX27) associates with zonula occludens-2 (ZO-2) and modulates the epithelial tight junction. *Biochem J.* **455**, 95–106.